See related commentary on pg 1855

Cell Death of Melanophores in Zebrafish *trpm7* Mutant Embryos Depends on Melanin Synthesis

Matthew S. McNeill[1], Jennifer Paulsen[2], Gregory Bonde[2], Erin Burnight[3], Mei-Yu Hsu[4] and Robert A. Cornell[1,2,3]

Transient receptor potential melastatin 7 (TRPM7) is a broadly expressed, non-selective cation channel. Studies in cultured cells implicate TRPM7 in regulation of cell growth, spreading, and survival. However, zebrafish *trpm7* homozygous mutants display death of melanophores and temporary paralysis, but no gross morphological defects during embryonic stages. This phenotype implies that melanophores are unusually sensitive to decreases in Trpm7 levels, a hypothesis we investigate here. We find that pharmacological inhibition of caspases does not rescue melanophore viability in *trpm7* mutants, implying that melanophores die by a mechanism other than apoptosis. Consistent with this possibility, ultrastructural analysis of dying melanophores in *trpm7* mutants reveals abnormal melanosomes and evidence of a ruptured plasma membrane, indicating that cell death occurs by necrosis. Interestingly, inhibition of melanin synthesis largely prevents melanophore cell death in *trpm7* mutants. These results suggest that melanophores require Trpm7 in order to detoxify intermediates of melanin synthesis. We find that unlike *TRPM1*, *TRPM7* is expressed in human melanoma cell lines, indicating that these cells may also be sensitized to reduction of TRPM7 levels.

Journal of Investigative Dermatology (2007) **127,** 2020–2030; doi:10.1038/sj.jid.5700710; published online 8 February 2007

INTRODUCTION

Genetic pathways that govern the survival of melanocytes are of interest in the etiology of depigmentation disorders like vitiligo, and in the design of new therapies for malignant melanoma. Molecular studies of the mouse ''white-spotting'' mutants, which have patches of skin devoid of melanocytes, have identified genes encoding proteins that regulate melanocyte survival (for instance, receptor tyrosine kinase, Kit, and transcription factors Mitf and Sox10, reviewed by Baxter *et al.*, 2004). In recent years, zebrafish and medaka mutants deficient in melanophores, the fish counterparts of melanocytes, have been isolated in mutagenesis screens or discovered in stock strains (Kelsh *et al.*, 1996; Lynn Lamoreux *et al.*, 2005). Of the melanophore-deficient zebrafish mutants that have been molecularly characterized, most harbor mutations in orthologs of genes disrupted in mouse white-spotting mutants, including *kit* (Parichy *et al.*, 1999), *mitf* (Lister *et al.*, 1999), and *sox10* (Dutton *et al.*, 2001). This finding supports the notion that melanocyte regulatory mechanisms are conserved between fish and mammals. This is important because many fish pigmentation mutants remain to be analyzed; continued molecular characterization of these mutants may yield unexpected insight into the genetic control of melanocyte development.

An example of an unexpected discovery from zebrafish is that the melanophore-deficient mutant *touchtone/nutria* (Arduini and Henion, 2004; Cornell *et al.*, 2004) corresponds to the *transient receptor potential melastatin 7* (*trpm7*) gene (Elizondo *et al.*, 2005), which was not previously implicated in melanocyte development. The transient receptor potential (TRP) family of ion channels includes 28 members in mammals, which are expressed in a variety of tissues and are implicated in a wide array of functions (reviewed by Ramsey *et al.*, 2006). The eight members of the TRPM (melastatin) subfamily share a set of structural motifs: a canonical amino-terminal domain, six transmembrane domains, and a conserved coiled-coil domain (reviewed by Harteneck, 2005). TRPM6 and TRPM7 additionally share the unusual feature of an intrinsic alpha-helix-directed kinase activity in the intracellular carboxy-terminal tail. The founding member of this family, TRPM1 (Melastatin), was identified by virtue of being expressed in benign nevi but not in metastatic melanoma (Duncan *et al.*, 1998); TRPM1 expression has been shown to be directly stimulated by MITF (Miller *et al.*, 2004; Zhiqi *et al.*, 2004), but the physiological function of MITF is unknown. TRPM7 is permeable to Ca^{2+}, Mg^{2+}, and trace ions (reviewed by Wolf, 2004) and is expressed in all or most cells of adult mice (Kunert-Keil *et al.*, 2006). Anti-TRPM7 antibody immunoreactivity has been detected at the

[1]*Interdisciplinary Graduate Program in Neuroscience, University of Iowa, Iowa City, Iowa, USA;* [2]*Department of Anatomy and Cell Biology, University of Iowa, Iowa City, Iowa, USA;* [3]*Interdisciplinary Graduate Program in Genetics, University of Iowa, Iowa City, Iowa, USA and* [4]*Department of Pathology, Brigham and Women's Hospital, Harvard Medical School, Boston, Massachusetts, USA*

Correspondence: Dr Robert A. Cornell, 1-532 BSB, University of Iowa, Iowa City, Iowa 52240, USA. E-mail: robert-cornell@uiowa.edu

Abbreviations: AO, acridine orange; cDNA, complementary DNA dct, dopachrome tautomerase; dpf, days post-fertilization; hpf, hours post-fertilization; trpm7, transient receptor potential melastatin 7

Received 18 August 2006; revised 21 October 2006; accepted 15 November 2006; published online 8 February 2007

plasma membrane of retinoblastoma cells (Hanano *et al.*, 2004), and in synaptic vesicles of sympathetic neurons (Krapivinsky *et al.*, 2006), but an extensive analysis of the subcellular localization of TRPM7 protein has not been reported.

To date, no mouse *Trpm7* mutant has been described, but depletion of the TRPM7 protein in cell lines has yielded insight into its role in various tissues. For example, small-interfering RNA-mediated knockdown of *TRPM7* in retinoblastoma and smooth muscle cell lines causes growth arrest (Hanano *et al.*, 2004; He *et al.*, 2005), and in fibroblasts causes increased spreading and cell adhesion, in part through calcium-dependent regulation of calpain (Su *et al.*, 2006). Trpm7 also appears to regulate contractility in mouse cells via calcium-dependent and kinase-dependent regulation of actomyosin (Clark *et al.*, 2006). Recent evidence implicates TRPM7 in release of acetylcholine from cultured sympathetic neurons (Krapivinsky *et al.*, 2006). In the DT-40 chicken B-lymphocyte cell line, mutation of *Trpm7* by homologous recombination causes growth arrest and cell death (Nadler *et al.*, 2001). Interestingly, the cell death observed in DT-40 B cells is completely reversed by the addition of 10 mM Mg^{2+} to the culture medium, leading to the suggestion that TRPM7 plays an essential role in the regulation of cellular magnesium homeostasis (Schmitz *et al.*, 2003). There is evidence that TRPM7 activity is regulated by intracellular Mg-ATP, PIP_2 hydrolysis, reactive oxygen species (whose levels it also modulates), and its intrinsic kinase domain (reviewed by Aarts and Tymianski, 2005; Harteneck, 2005; McNulty and Fonfria, 2005; Scharenberg, 2005; Miller, 2006).

Given evidence that TRPM7 is required for growth, adhesion, and/or survival in different cell types, and the observation that the *trpm7* transcript is expressed broadly in zebrafish embryos (Thisse *et al.*, 2001), one might have expected a gross morphological phenotype involving widespread cell death or dysmorphogenesis in zebrafish *trpm7* mutant embryos. Instead, embryos homozygous for a strong hypomorphic or null allele of *trpm7* appear equivalent to siblings up until approximately 30 hours post-fertilization (hpf), when it becomes apparent that cutaneous melanophores in the mutants are reduced in size and number compared to those of their siblings (i.e., wild types and *trpm7* heterozygotes) (Arduini and Henion, 2004; Cornell *et al.*, 2004). Analysis of *dopachrome tautomerase* (*dct*) expression at 28 hpf in *trpm7* mutants revealed that normal numbers of melanoblasts are specified, but by 48 hpf melanophores and undifferentiated melanoblasts are virtually absent, suggesting wholesale death of this developing cell population (Arduini and Henion, 2004; Cornell *et al.*, 2004). In addition, whereas mutant embryos move spontaneously and respond to touch just like wild-type embryos at 28 hpf, they fail to swim away in response to a mild tap at 48 hpf. It is important to note that defects in pigmentation and behavior are readily observed, and there may be other cryptic defects in these mutants; nonetheless, the absence of widespread cell death or growth arrest implies that a compensatory activity is present in early *trpm7* mutants (i.e., an embryonic-stage Trpm7 compensatory activity). This compensatory activity may be provided by Trpm7 encoded by maternal transcripts. Maternal transcripts have been observed to compensate for a lack of zygotic transcripts during the first few days of development in other zebrafish mutants (Gritsman *et al.*, 1999; Giraldez *et al.*, 2005; Kane *et al.*, 2005), and we detect high levels of maternal *trpm7* transcripts (M.S.M. and R.A.C., unpublished data). Alternatively, the compensatory activity in early embryos may be the product of another gene, presumably also an ion channel. A trivial explanation for melanophore cell death in *trpm7* mutants is that the hypothetical compensatory activity is not expressed in melanophores; alternatively, melanophores have an increased dependence on Trpm7 relative to other cell types because of their unique metabolic properties, which is the hypothesis we test in this study.

Unexpectedly, at about 72 hpf, melanophores begin to appear in *trpm7* mutants, and the animals regain touch responsiveness. The recovery of these defects strongly suggests that at this stage a gene product providing Trpm7-like activity, perhaps a Trpm7 homolog, becomes expressed in melanophores and in the unknown cells responsible for paralysis. This larval stage Trpm7 compensatory activity does not compensate for the lack of Trpm7 in all cells, however, because by 7 days post-fertilization (dpf), *trpm7* mutants display delayed growth and abnormal skeletal calcification, presumed to reflect abnormal kidney function (Elizondo *et al.*, 2005). Because the identity of the putative larval stage Trpm7 compensatory activity is currently unknown, this study was confined to exploring the mechanism of melanophore cell death in embryonic *trpm7* mutants. We find evidence that melanophores undergo necrotic death in *trpm7* mutants, but that inhibition of melanin synthesis utterly prevents it, suggesting a new method to target cell death to melanized cell types.

RESULTS

Melanophore cell death in *trpm7* mutants is rescued by increased magnesium

To investigate the mechanism of melanophore death in *trpm7* mutant embryos, we tested a variety of compounds for their ability to prevent it. In *trpm7* mutant embryos, a few pale melanophores are usually detectable at 48 hpf. We have previously found that adding magnesium or calcium to the medium in which mutants were raised moderately increased the size and extent of melanization in some melanophores (Elizondo *et al.*, 2005). To test whether supplemental magnesium would also prevent melanophore death in *trpm7* mutants, we counted melanophores in mutants raised in embryo medium supplemented with 100 mM magnesium chloride. In five experiments, we detected a variable but usually significant increase in the number of viable-looking melanophores in magnesium-treated *trpm7* mutants (Table 1). To test the hypothesis that altered calcium homeostasis contributes to melanophore cell death in *trpm7* mutants, we raised embryos in embryo medium supplemented with 50 or 100 mM calcium chloride. In multiple experiments, we did not detect a change in the number or quality of melanophores in mutant embryos raised in calcium using the highly

Table 1. Numbers of melanophores in *trpm7* mutant embryos raised in supplemental magnesium

	Wild-type	*trpm7* $^{-/-1}$	*trpm7* $^{-/-}$	*trpm7* $^{-/-}$
Supplemental $MgCl_2$[2]	0	0	50 mM	100 mM
Total melanophores[3]	50.7 (7.9)	1.4 (1.4)	3.3 (2.0)	8.1 (3.1)
Avg. (SD)			P=0.153[4]	P=0.001[4]
n (Number of embryos scored)	10	10	9	8

[1]The *trpm7*^{b508} allele, a strong hypomorph or null allele, was used in this experiment.
[2]All embryos were incubated in 10% Hank's solution (Westerfield, 1993), which contains 0.1 mM $MgSO_4$ and 0.13 mM $MgCl_2$.
[3]Melanophores were counted on the dorsal aspect of the embryo between two clear morphological landmarks, the caudal aspect of the eyes and the point where the hindbrain constricts to form the spinal cord, around the position of the second somite.
[4]Two-tailed Student's *t*-test, compared to *trpm7* mutants with no supplemental magnesium.
The results of this experiment were variable. In individual experiments with 100 mM $MgCl_2$, and at least eight embryos counted per treatment, significant rescue of 9.3% (shown in this Table), 3.7%, and 7.7%, was observed, but twice no significant rescue was observed (see Materials and Methods for formula used to calculate rescue efficiency).

penetrant *trpm7*^{b508} allele or the less penetrant *trpm7*^{b722} (not shown). Of note, improved morphology of melanophores in *trpm7*^{b508} mutants raised in elevated calcium has been repeatedly observed in two other laboratories in which this strain is maintained, although this effect is widely variable (David Parichy and Paul Henion, personal communication). We cannot currently explain the variability between laboratories in the effectiveness of this experiment; relevant parameters may include the genetic background in which the mutant is carried and trace ions present in fish water.

Melanophore cell death is not rescued by p53 inhibition

We reasoned that as TRPM7 inhibition causes growth arrest in some cultured cells (Hanano *et al.*, 2004), perhaps the observed cell death of melanophores in *trpm7* mutants is triggered by the p53-mediated checkpoint response. To test this possibility, we used a previously described antisense morpholino oligonucleotide (MO) targeting the *p53* transcript to knock down p53 expression (Langheinrich *et al.*, 2002). Zebrafish embryos injected with the *p53* MO resist cell death induced by camptothecin, a DNA topoisomerase inhibitor, until 24 hpf (Langheinrich *et al.*, 2002). We first tested whether the *p53* MO is still effective at 36 hpf, a stage by which the phenotype of abnormal melanophores is obvious in *trpm7* mutants. We injected wild-type embryos with *p53* MO shortly after fertilization, added camptothecin at 32 hpf, and assessed cell death at 36 hpf using the acridine orange (AO) exclusion assay. Untreated control embryos displayed AO-positive cells in the nasal placode, reflecting developmentally regulated cell death in that tissue (Cole and Ross, 2001), but otherwise exhibited only a few scattered AO-positive cells (Figure 1a). Addition of camptothecin led to an obvious increase in AO-positive cells in uninjected controls (Figure 1b) but not in *p53* MO-injected embryos (Figure 1c), confirming that MO-mediated inhibition of p53 perdures until the stage when melanophores die in *trpm7* mutants. Next, we injected embryos derived from *trpm7* heterozygous fish with *p53* MO, and counted melanophores at 48 hpf. We did not detect differences in melanophore number, or morphology of melanophores, between the MO-injected and uninjected mutant embryos (Figure 1e and f). To test the possibility that undifferentiated melanoblasts were present in *p53* MO-injected mutants, we processed such embryos to reveal expression of the melanoblast-specific marker *dopachrome tautomerase* (*dct*) (Kelsh *et al.*, 2000). Unmelanized, *dct*-expressing cells were not detected in either treated or untreated mutant embryos at 48 hpf (not shown). These findings indicate that cell death of melanophores in *trpm7* mutants does not depend on p53.

A broad-spectrum caspase inhibitor rescues melanophore viability in *kit* but not *trpm7* mutant embryos

Kit is a receptor tyrosine kinase expressed in melanocytes whose signaling via the MAP kinase cascade and the transcription factor Mitf promotes expression of the anti-apoptotic protein Bcl2 (Hemesath *et al.*, 1998; McGill *et al.*, 2002). In zebrafish *kit* mutants, embryonic melanophores undergo cell death and express the marker of apoptosis, TUNEL (Parichy *et al.*, 1999). By contrast, TUNEL-positive melanophores were not detected in *trpm7* mutants, suggesting that these cells die by a mode other than apoptosis (Arduini and Henion, 2004; Cornell *et al.*, 2004). The best-studied form of apoptosis is caspase dependent, and the broad-spectrum caspase inhibitor zVAD-fmk has been shown to inhibit developmentally programmed cell death in zebrafish embryos (Williams and Holder, 2000; Williams *et al.*, 2000; Sanders and Whitlock, 2003). To test whether melanophores in *trpm7* mutants undergo caspase-dependent apoptosis, we tested the effects of zVAD-fmk in these mutants. As a positive control, *kit* mutant embryos were incubated in fish water supplemented either with 300 μM zVAD-fmk or the related compound zFA-fmk, which does not target caspases (Williams *et al.*, 2000). The presence of zVAD-fmk, but not zFA-fmk, increased the number of viable melanophores in *kit* mutants at 5 dpf, indicating that melanophore death in *kit* mutants is caspase-dependent (Figure 1i and j, and not shown). Next, we incubated embryos derived from *trpm7* heterozygous mutant zebrafish in fish water with or without zVAD-fmk. However, at 48 hpf, zVAD-fmk-treated mutants appeared equivalent to untreated mutants (Figure 1e and g), and we confirmed this by counting melanophores at 5 dpf (Figure 1, lower histogram). We also

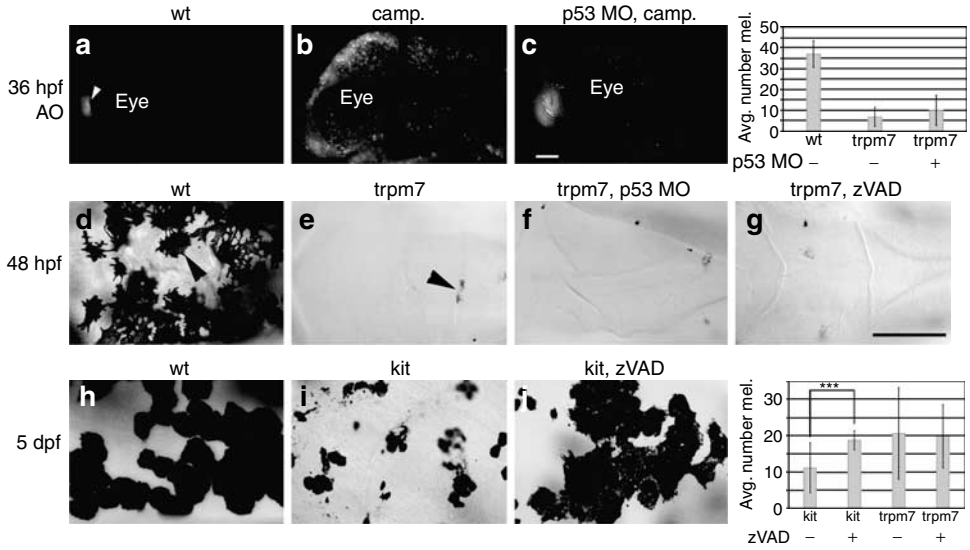

Figure 1. Inhibitors of p53 or caspases do not rescue melanophore death in *trpm7* mutant embryos. (**a**–**c**) Lateral views of 36 hpf embryos processed with AO to reveal dying cells. (**a**) In a wild-type (*wt*), untreated embryo, very few dying cells are detected except in the olfactory placode (arrowhead). (**b**) In a wild-type embryo that was treated with cell-cycle inhibitor camptothecin (camp.) at 32 hpf, large numbers of dying cells are visible in proliferative areas of the brain at 36 hpf. (**c**) In a wild-type embryo injected with *p53* MO and treated with camptothecin, many fewer dying cells are seen than in (**b**). (**d**–**j**) Dorsal views of the heads of live embryos of the indicated genotypes, for (**d**–**g**) at 48 hpf, and for (**h**–**j**) at 5 dpf. (**d**) A wild-type embryo where individual melanophores (arrowhead) are black, dendritic, and abundant in number. (**e**) An uninjected *trpm7* mutant embryo in which melanophores are small, pale, and highly reduced in number (arrowhead). (**f**) A *p53* MO-injected *trpm7* embryo; melanophores resemble those in uninjected mutants. (**g**) A *trpm7* mutant raised in the presence of 300 μM zVAD-fmk; no change in number or morphology of melanophores is apparent. (**h**) In a wild-type embryo at 5 dpf, melanophores are large, black, but not dendritic. (**i**) In an untreated *kit* mutant, constricted, black melanophore corpses are visible (Parichy *et al.*, 1999). (**j**) In a *kit* mutant raised in the presence of the pan-caspase inhibitor zVAD-fmk, many melanophores display a normal morphology. Histograms: top, number of melanophores in *wt* and uninjected versus *p53* MO-injected *trpm7* mutant embryos at 48 hpf. Bottom, number of melanophores in *kit* and *trpm7* mutant embryos, with or without addition of caspase inhibitor zVAD-fmk, at 5 dpf. Asterisks indicate significant difference, *t*-test, $P<0.01$. Numbers of embryos counted were *kit*, $n=10$; *kit*+zVAD, $n=10$; *trpm7*, $n=5$; *trpm7*+zVAD, $n=11$. p53 MO and zVAD-fmk were tested for their ability to rescue melanohores in both weaker (i.e., $trpm7^{b722}$) and stronger (i.e., $trpm7^{b508}$ or tdo^{tz310c}) alleles. In this Figure, $trpm7^{b722}$ was used for the *p53* MO experiment and tdo^{tz310c} was used for zVAD-fmk experiment. Bars = 100 μm. Bar in (**c**) applies to (**a**–**c**). Scale bar in (**g**) applies to (**d**–**j**).

failed to detect unpigmented *dct*-expressing cells zVAD-fmk-treated mutant embryos (not shown). Overall, these results indicate that melanophore cell death in *trpm7* mutant embryos does not depend on zVAD-fmk-sensitive caspases.

In *trpm7* mutants, embryonic melanophores exhibit features of non-apoptotic cell death

Distinct modes of cell death are most reliably distinguished by the morphology of the dying cell (Kerr *et al.*, 1972) (reviewed by Assuncao Guimaraes and Linden, 2004). We used transmission electron microscopy to investigate melanophore ultrastructure in wild types, $trpm7^{b722}$ mutants, and, as a positive control for apoptosis, the *kit* mutant. (We used the $trpm7^{b722}$ mutants in this experiment because in them melanophores tend to have more melanin and are thus easier to detect than in $trpm7^{b508}$ mutants). In wild-type embryos at 48 hpf, melanophores were flat and dendritic, and most often present just basal to the basement membrane of the epidermis (Figure 2a and not shown). Melanosomes were round and electron dense, with sharp boundaries (Figure 2b). In *trpm7* mutants at 48 hpf, melanophores were also beneath the basement membrane, but were neither as flat nor as extended as their wild-type counterparts (Figure 2c). Many melanosomes in these cells had irregular boundaries, revealing abnormal deposition of melanin on the melanosome matrix (Figure 2d). Interestingly, melanosomes in the melanophores of *trpm7* mutants were occasionally detected in tissue surrounding the presumptive melanophore (Figure 2e, $n=2$ of 9 cells examined by transmission electron microscopy), providing strong evidence that the plasma membrane of these cells had ruptured. We did not detect free melanosomes in sections of wild-type embryos ($n=8$ cells examined). For comparison, we assessed the morphology of melanophores in *kit* mutants at 5 dpf, the stage at which the highest fraction of melanophores has been found to be TUNEL positive (Parichy *et al.*, 1999). In contrast to what was seen in *trpm7* mutants, melanophores in *kit* mutants were observed being extruded through the skin, as previously reported (Figure 2f) (Parichy *et al.*, 1999), and melanosomes were never found outside of the melanophores ($n=7$ melanophores examined). Moreover, the melanosomes in *kit* mutants had sharp boundaries (Figure 2g). In summary, melanophores in *trpm7* and *kit* mutants exhibited distinct morphologies, suggesting that *trpm7* mutant melanophores die by a mechanism other than apoptosis.

Melanophore cell death in *trpm7* mutant embryos is dependent on melanin synthesis

The conversion of tyrosine to L-DOPA begins a biochemical cascade to form melanin yielding quinone and indole

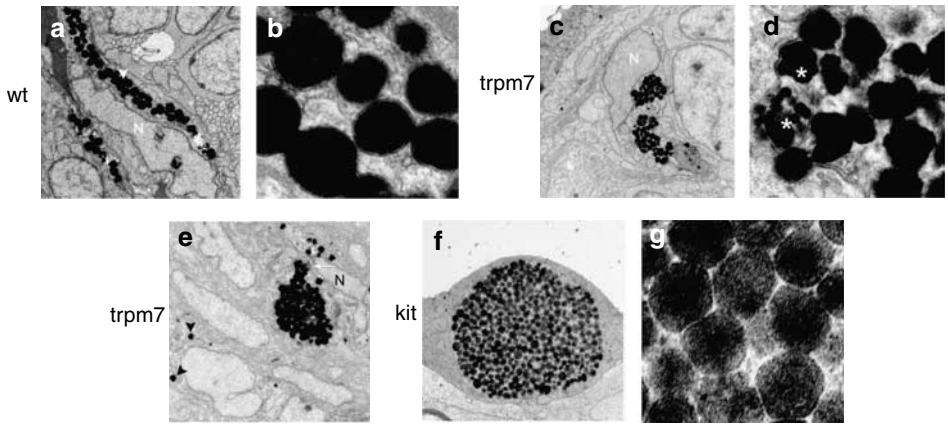

Figure 2. The melanophore ultrastrucure in *trpm7* and *kit* mutants is distinct. (**a**) A melanophore in a wild-type embryo at 48 hpf. The melanophore is extended and has a linear arrangement of melanosomes (white arrowhead) surrounding an intact nucleus (N). (**b**) High magnification view of melanosomes shown in (**a**). Melanosomes are highly electron dense with smooth edges. (**c**) A melanophore in a *trpm7* mutant embryo at 48 hpf. The melanophore is not extended, and has clumped groups of melanosomes. (**d**) High magnification view of melanosomes in (**c**), which are electron dense but have abnormal shape and do not always appear to have a vesicular membrane (*). (**e**) A second melanophore in a *trpm7* mutant embryo, for which the cellular membrane appears to have ruptured (white arrow). Melanosomes can be seen in the extracellular space near this cell (black arrowheads). (**f**) In a *kit* mutant at 5 dpf a melanophore, or a macrophage-engulfed corpse of a melanophore, as it is extruded through the skin of the embryo (asterisk is in extra embryonic space). (**g**) High magnification view of melanosomes within melanophore shown in (**f**), which appear intact but are less electron dense than those in wild-type embryos at 48 hpf. Bar (**a**) = 1 μm (**a**, **c**, **e**, and **f**), (**b**) = 200 nm (**b**, **d**, and **g**).

intermediates, compounds that have the potential to become cytotoxic (Riley, 1998; Mastore *et al.*, 2005). To test the hypothesis that intermediates of melanin synthesis contribute to melanophore death in *trpm7* mutant embryos, we applied 1-phenyl-2-thiourea (PTU), a copper chelator that effectively inhibits the copper-dependent enzyme Tyrosinase, to a clutch of embryos derived from *trpm7*^{b508} heterozygotes. At 48 hpf, homozygous mutants were separated from the rest of the clutch based upon their paralysis phenotype, fixed and processed to reveal *dct* expression. As expected, untreated embryos exhibited a strong reduction of *dct*-expressing cells at 48 hpf (Figure 3a, b, and i). By contrast, all PTU-treated embryos had a normal complement of *dct*-positive cells (Figure 3c, d, and i), suggesting that inhibition of melanin synthesis prevents melanophore cell death in *trpm7* mutants. PTU did not reduce cell death in *kit* mutants (not shown), indicating that cell death in this mutant is not dependent upon melanin production (not shown).

To further test the hypothesis that melanophore death in *trpm7* mutants is caused by melanin synthesis, as opposed to by some other function of Tyrosinase, we tested whether two zebrafish strains that express unusually low levels of melanin, but are not *tyrosinase* mutants, are protected from melanophore cell death induced by *trpm7* dysfunction. Zebrafish *albino* mutant embryos and adults have no visible melanin in either their melanophores or retinal pigmented epithelium; the *albino* locus has not been molecularly characterized but it resides on a different chromosome from *tyrosinase* (i.e., *albino*, chromosome 21, *tyrosinase*, chromosome 15, Postlethwait *et al.*, 1994; Page-McCaw *et al.*, 2004). We generated adults heterozygous for both *albino* and *trpm7*^{b722}, crossed them and identified double homozygotes from among their progeny at 48 hpf. This selection was based on paralysis and an absence of melanin in the eye (*albino* homozygotes are touch responsive, *trpm7* homozygotes have black eyes). We fixed and processed all embryos to reveal *dct* expression. We detected no reduction of *dct*-positive cells in *albino*/*trpm7* double-mutant embryos as compared to homozygous *albino* siblings (Figure 3e, f, and i). Because *trpm7*^{b722} in some experiments displays a less penetrant phenotype of melanophore death than other *trpm7* alleles, we confirmed the finding by injecting a MO targeting the *trpm7* transcript into *albino* mutants. First we confirmed that wild-type embryos injected with *trpm7* MO had a strong reduction of melanophores at 48 hpf similar to *trpm7* mutants, as we have shown previously (Figure 3, histogram; Elizondo *et al.*, 2005). However, *albino* mutant embryos injected with *trpm7* MO had a normal complement of *dct*-positive cells, confirming the finding in double mutants (not shown).

Zebrafish *golden* mutant embryos have pale melanophores, owing to low melanin density and a reduced number of melanosomes (Streisinger *et al.*, 1981; Lamason *et al.*, 2005). *Golden* corresponds to the gene encoding SLC24A5, a putative Na^+/H^+ cation exchanger expressed on an intracellular compartment presumed to be the melanosome (Lamason *et al.*, 2005). To test whether knockdown of *trpm7* expression would cause melanophore cell death in *golden* mutants, we injected embryos derived from *golden* homozygous adults with a control MO or *trpm7* MO and counted melanophores at 48 hpf. However, injection of *trpm7* MO into *golden* mutant embryos did not change the number of melanophores detected at 48 hpf relative to the number seen in *golden* mutant embryos injected with control MO (Figure 3g–i). These results, along with those obtained using *albino* mutants, suggest that melanophore death occurs in *trpm7* mutants only if melanin synthesis is greater than a threshold level.

Embryonic melanophores lose their dependence on Trpm7

Whereas normal-looking melanophores are absent from *trpm7* mutants at 48 hpf, they begin to reappear starting

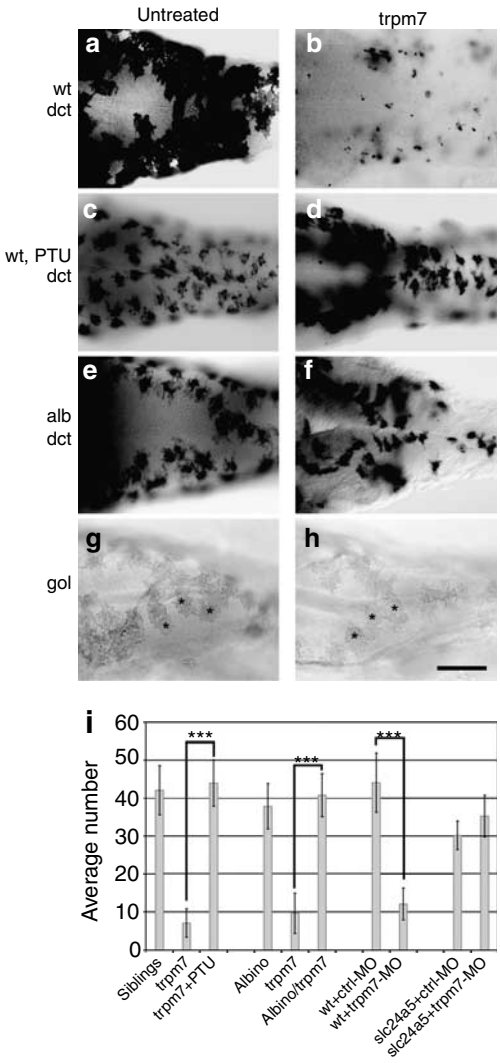

Figure 3. Inhibition of melanin synthesis rescues melanophore death in *trpm7* mutants. Dorsal views of heads of 48 hpf embryos of the indicated genotypes, processed to reveal *dct* expression (except (**g** and **h**), which are unprocessed). (**a**) In a wild-type embryo, melanophores are abundant. (**b**) In a *trpm7* mutant, melanophores are small, puctate or absent. Unpigmented, *dct*-expressing cells are not detected. (**c**) In a wild-type embryo treated with the tyrosinase inhibitor PTU, melanophores are unpigmented but can be identified by their expression of *dct*. (**d**) In a PTU-treated *trpm7* mutant, *dct*-expressing cells are abundant. (**e**) An *albino* (*alb*) mutant with abundant, unpigmented, but *dct*-expressing melanophores. (**f**) An *albino/trpm7* double mutant, also with abundant *dct*-expressing melanophores. (**g**) An *slc2485/golden* mutant embryos injected with a control MO, showing lightly pigmented melanophores (asterisks) (Lamason *et al.*, 2005). (**h**) A *trpm7* MO-injected *slc2485/golden* mutant embryo, with comparable number of melanophores as uninjected controls. (**i**) Histogram showing the average number of melanophores in each treatment group. *Significant difference, *t*-test, $P<0.01$. Error bars indicate 1 SD. Embryos counted: siblings, $n=11$; *trpm7* $n=11$; *trpm7* + PTU, $n=12$; *albino* $n=8$; *trpm7* $n=8$; *trpm7/albino* $n=5$; *wt* + ctrl MO, $n=10$; *wt* + *trpm7* MO = 11; *gol* + ctrl MO, $n=11$; *gol* + *trpm7* MO = 11. Bar = 100 μm in all panels.

around 72 hpf (Arduini and Henion, 2004; Cornell *et al.*, 2004). It was recently shown that after all melanophores in wild-type zebrafish embryos are killed using a specific toxin that is subsequently washed off, new melanophores emerge from stem cells (Yang and Johnson, 2006). It thus seems probable that the melanophores that repopulate *trpm7* mutants at around 72 hpf are derived from this stem cell population, although some may derive from clonal growth of rare embryonic melanophores that survive through the early period. To explain the reemergence of melanophores after 72 hpf, we considered two models. In one, embryonic melanophores depend on Trpm7 whereas stem-cell-derived melanophores do not. In the second, melanophores, regardless of origin, depend on Trpm7 if they differentiate before 48 hpf but not if they do so later than 72 hpf. A prediction of the first model is that if differentiation (melanization) of embryonic melanophores were to be delayed until after 72 hpf, these melanophores would nevertheless die. If the second model is correct, these cells will survive. We treated a clutch of *trpm7* mutant embryos with a low dose of PTU, which allowed melanophores to become pigmented to approximately the level seen in *golden* mutants. As expected, at 48 hpf the homozygotes – as identified by paralysis – had numbers of (pale) melanophores comparable to those of their motile, non-mutant siblings. We then washed the PTU from these embryos and observed their melanophores every 12 hpf for the next 4 days. As the melanophores became progressively darker, they adopted the large, extended morphology of healthy melanophores rather than dying (not shown). These results support our second model, according to which embryonic melanophores lose their dependence on Trpm7 at around 3 dpf, presumably because a homologous protein is expressed at this time (i.e., the larval-stage Trpm7 compensatory activity). This putative activity may be expressed broadly, as is Trpm7, because the embryos also recover from paralysis at this time.

TRPM7 is expressed in metastatic melanoma cell lines

Our finding that zebrafish melanophores have a heightened dependence on Trpm7 activity suggested that melanoma cells, which can be highly pigmented, might share this feature. However, it is known that TRPM1, a member of the TRP channel subgroup to which TRPM7 belongs, is expressed at high levels in benign nevi but at low levels in metastatic melanoma cells (Duncan *et al.*, 1998). To learn whether the expression of *TRPM7* is regulated in a manner similar to that of *TRPM1*, we used quantitative RT-PCR to assess the levels of *TRPM1* and *TRPM7* transcripts present in several cell lines. We first confirmed that, as previously reported, *TRPM1* levels are high in a normal melanocyte cell line (FM13), but very low in three cell lines derived from melanoma (cell lines WM983A, A375P, and WM1205Lu) (Figure 4). By contrast, we found that *TRPM7* levels are comparable in normal melanocytes (FM13), fibroblasts (DF1), keratinocytes (FK10), and present at relatively high levels in WM1205Lu, A375P cells, and WM983A (Figure 4). Moreover, *TRPM7* message levels remained high in subpopulations of A375P selected for invasive behavior in an *in vitro* invasion assay (A375P-5 and A375P-10) (Seftor *et al.*, 1990) and for metastatic potential in mice (A375M) (Figure 4), whereas *TRPM1* expression was low or absent from these lines. These results suggest that, in contrast to *TRPM1*, *TRPM7* is expressed in metastatic melanoma. This is consistent with

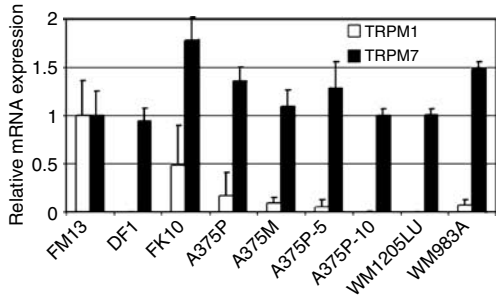

Figure 4. Comparison of *TRPM7* and *TRPM1* messenger RNA levels in several human cell lines. *TRPM7* expression was comparable in three control cell lines: melanocytes (FM13), dermal fibroblasts (DF1), and somewhat higher in keratinocytes (FK10). Similar expression levels were detected in the metastatic melanoma cell line A375P and its invasive variants selected in an *in vitro* invasion assay (A375P-5 and A375P-10) or a murine tumor-forming assay (A375M) (Seftor *et al.*, 1990). Levels were also similar in melanoma (WM983A) and metastatic melanoma cell lines derived from a primary tumor (WM1205Lu). *TRPM1* messenger RNA expression levels were high in melanocytes (FM13), but were decreased or absent in dermal fibroblasts (DF1), keratinocytes (FK10), and all melanoma cell lines.

the possibility that, like zebrafish embryonic melanophores, melanoma cells may have a heightened dependence on TRPM7 relative to other cell types.

DISCUSSION

Melanophore cell death in *trpm7* mutants depends on melanin synthesis

Based on differences in the features of melanophore cell death in *kit* and *trpm7* mutants, we propose that in the latter, at least a majority of melanophores die by necrosis. Kit signaling is necessary for the survival of melanocytes because it promotes expression of the antiapoptotic factor Bcl2 (Hemesath *et al.*, 1998; McGill *et al.*, 2002). By contrast, Trpm7 appears to be required to prevent an accumulation of cytotoxic intermediates of melanin synthesis, which eventually cause death by necrosis. Melanin synthesis begins with oxidation of the metabolic precursor L-tyrosine by the enzyme tyrosinase, and proceeds through indole and orthoquinone intermediates, which may be highly toxic owing to their ability to be converted to semiquinone-free radicals and other reactive oxygen species (Hochstein and Cohen, 1963; Pawelek and Lerner, 1978). Tyrosinase-dependent death of cutaneous melanocytes is also seen in mouse *tyrosinase-related protein 1* mutants (Johnson and Jackson, 1992) and of choroidal melanocytes in mouse *tyrosinase-related protein 1/Gpnmb* mutants (Anderson *et al.*, 1990). In the reports of these findings, the mode of cell death was not assessed. Depigmenting agents such as 4-hydroxyanisole and other phenolic or catecholic compounds are converted by tyrosinase to orthoquinones (reviewed by Huang *et al.*, 2002), and recently, one such compound, (2 morpholinobutyl)-4-thiophenol, was demonstrated to cause melanophore cell death in zebrafish embryos (Yang and Johnson, 2006). In this study, it was noted that melanophore corpses are extruded through the skin, as in *kit* mutants, perhaps indicating apoptotic cell death. Consistent with this possibility, 4-tertiary butylphenol was seen to induce apoptosis in cultured melanocytes (Yang *et al.*, 2000). In contrast, chemotherapy treatment of melanoma has been observed to result in extracellularly localized melanosomes, indicative of necrosis (Busam *et al.*, 2004). Whether a cell dies by apoptosis or necrosis is dependent on the availability of ATP, with lower levels favoring necrosis (Nicotera and Melino, 2004). Interestingly, magnesium is a required ATP cofactor, so it is conceivable that reduced magnesium effectively diminishes the available pool of ATP in *trpm7* mutants and biases melanophores towards necrosis. Rare melanophores positive for anti-activated caspase-3 immunoreactivity are detected in *trpm7* mutants (Arduini and Henion, 2004), suggesting that some fraction of melanophores most likely undergo apoptosis.

Which of Trpm7's potential functions is essential to detoxify or prevent the accumulation of intermediates produced during melanin synthesis? Trpm7 channels are permeable not only to abundant cations such as calcium and magnesium, but also to trace ions such as zinc, copper, and manganese (Monteilh-Zoller *et al.*, 2003). Additionally, they contain an intrinsic kinase activity. We found that supplemental magnesium could variably rescue a small fraction of melanophores from cell death in *trpm7* mutants. This effect was far less impressive than the complete prevention of cell death achieved by supplementing DT-40 B-lymphocytes homozygous for *TRPM7* deletion with magnesium (Schmitz *et al.*, 2003), but in fish embryos, organism-level physiology may limit the levels of magnesium to which melanophores are exposed. It is also possible that the essential detoxifying role of Trpm7 in melanophores is mechanistically unrelated to the essential requirement of TRPM7 in B cells and other cell types. For instance, a magnesium-dependent enzyme that is necessary in melanophores but not in B cells is catechol-*o*-methyl-transferase, which methylates DOPA quinone and reduces its toxicity in melanocytes (Smit *et al.*, 1994). However, we found that addition of catechol-*o*-methyl-transferase inhibitor OR-486 at 50 μM, the highest non-toxic dose, did not selectively induce melanophore cell death in zebrafish embryos (M.S.M. and R.A.C. unpublished), suggesting that there may be other Trpm7-dependent enzymes involved in the detoxification of melanin synthesis intermediates. It is also noteworthy that supplemental calcium has been observed to variably rescue melanophores in *trpm7* mutants (Elizondo *et al.*, 2005). As with magnesium rescue, the reason for the variability of this effect is unclear; however, the ability of calcium to prevent melanophore cell death in *trpm7* mutants is consistent with the long-standing observation that calcium homeostasis is linked to both apoptotic and necrotic forms of death (Rizzuto *et al.*, 2003). Of note, there is evidence that the capacity of TRPM7 to activate m-calpain, thereby degrading focal adhesions, as well as TRPM7 kinase activity are mediated by calcium influx through TRPM7 (Su *et al.*, 2006). However, when melanoblast cell death in *trpm7* mutants is prevented by reducing melanin synthesis, the morphology of melanoblasts is not grossly more or less dendritic than melanoblasts in wild-type animals, although subtle differences may exist. This suggests that calcium-mediated mechanisms by which TRPM7 regulates melano-

phore viability are distinct from those by which it regulates cell spreading.

Trpm7 as a drug target

Is TRPM7 worth considering as a target for depigmenting agents? The presence of tyrosinase in melanoma cells has long been discussed as a potential ''Achilles heel'' by which they may be destroyed (Riley, 2003). Clinical trials of a tyrosinase substrate pro-drug were discontinued because of tyrosinase-independent side effects in the hepatocytes (Moridani *et al.*, 2002), emphasizing the need to consider other means to target cell death to tyrosinase-containing cells. We have shown that in early zebrafish embryos, melanophores are more sensitive to loss of Trpm7 than most other cell types, and we suggest this quality may be shared by melanoma cells where TRPM7 is expressed. One caveat is that there may be unidentified defects in embryonic *trpm7* mutants, and severe skeletal dysmorphogenesis likely resulting from abnormal kidney function is apparent in adult stage mutants (Elizondo *et al.*, 2005). Therefore, any therapeutic exploitation of the heightened sensitivity of melanocytes, and perhaps melanoma cell, to inhibition of TRPM7 will necessitate finding ways to limit these effects.

We note that in apparent contradiction to our model, melanophores appear normal in *trpm7* mutants at adult and larval stages. However, our finding that temporarily delaying melanization until after 48 hpf prevents cell death of embryonic melanophores strongly implies that a protein with redundant function is expressed in melanophores by this stage. The identity of this putative protein is unknown, but because its function seems to replace that of Trpm7, it is most likely a homolog of Trpm7. Thus we propose that careful modulation of TRPM7-type activity, which in zebrafish adults is possibly mediated by more than one Trpm7 homolog, may be selectively toxic only to melanized cell types. Plasma membrane-embedded ion channels like TRPM7 are attractive drug targets, and drugs that do not enter the cell would be expected to resist the recently described ability of melanosomes to chelate chemotherapeutic drugs (Chen *et al.*, 2006). Additionally, potential adverse effects in catecholaminergic neurons (discussed below) might be avoided with drugs impermeable to the blood–brain barrier.

Trpm7 and disease

We suggest that TRP family members should be considered as susceptibility genes for diseases characterized by the death of melanocytes or catecholaminergic neurons. Contact vitiligo is a genetically determined disease in which melanocyte death is triggered by exposure to phenolic compounds (Boissy and Manga, 2004). Although no known vitiligo susceptibility locus is found on chromosome 15 with *TRPM7* (Spritz, 2006), it is possible that a distinct TRP channel plays an analogous role in mammalian melanocytes. Supporting this possibility, mice that are heterozygous for mutation of the *mucolipin3* gene, a member of the TRP mucolipin subfamily (i.e., TRPML3), suffer loss of melanocytes and, interestingly, display reduced movement like zebrafish *trpm7* mutants (Cools, 1972; Di Palma *et al.*, 2002). Finally, a partial loss of function mutation of *TRPM7* has been correlated with a form of parkinsonism dementia (Hermosura *et al.*, 2005), a disease characterized by decreased function or survival of dopaminergic neurons. Zebrafish *trpm7* mutant embryos exhibit paralysis, but the cellular basis of this phenotype is unknown (Arduini and Henion, 2004; Cornell *et al.*, 2004). Paralysis in *trpm7* mutants may result from defects at the neuromuscular junction, as suggested by recent evidence that TRPM7 facilitates neurotransmitter release at cholinergic synapses (Krapivinsky *et al.*, 2006). However, it is noteworthy that biosynthesis of dopamine and other catecholamines is related to that of melanin. Thus it is an intriguing possibility that paralysis of zebrafish *trpm7* mutants results from a failure of Trpm7-dependent detoxification of dopamine synthesis.

MATERIALS AND METHODS

Animal husbandry and mutant alleles

Zebrafish were reared under the supervision of the University of Iowa Animal Care Unit, and all animal protocols were approved by the IACUC and comply with USDA laws and PHS Guidelines. Embryos were generated and handled following methods described by Westerfield (1993), and staged by hpf at 28.5°C (Kimmel *et al.*, 1995). Except as noted, experiments were conducted with the molecularly characterized allele $trpm7^{b508}$, which is highly penetrant (Elizondo *et al.*, 2005). *Touchdown* (tdo^{tz310c}) (Kelsh *et al.*, 1996), which has a highly penetrant phenotype indistinguishable from $trpm7^{b508}$ mutants or *trpm7* MO-injected embryos, was found to not complement $trpm7^{b508}$ and thus is most likely to be an allele of *trpm7*. $Trpm7^{b722}$, a more variable and sometimes less penetrant allele was used in some experiments as indicated. $Golden^{b1}$, $albino^{b2}$, and kit^{b5} alleles were used. Fish water, in which all adults and embryos were raised unless other specified, is distilled water further purified by reverse osmosis then supplemented with 0.30 g Crystal Sea® Marinemix (Marine Enterprises International; Baltimore, MD) per liter. Embryo media was prepared as described (Westerfield, 1993).

Morpholinos

Antisense MOs (Gene Tools; Sumerton, OR) were injected at a concentration of 0.4 mg/ml in a volume of 5 nl at the 1–4 cell stage. To target the *p53* transcript, we used a MO targeting the 5′UTR of the *p53* messenger RNA, which was shown previously to be effective and specific (Liu *et al.*, 2003) (i.e., *p53* MO2). The sequence of this oligonucleotide is 5′-GCG CCA TTG CTT TGC AAG AAT TG-3′. To target the *trpm7* message, we used a MO we have previously shown to effectively block splicing at the exon 12, intron 12 junction (Elizondo *et al.*, 2005). The sequence of this MO is 5′-GTG TGT GAG ATT TAC TCT GCT GTT C-3′. The standard control MO from Gene Tools was used as a negative control.

Histology

Embryos were fixed and processed for whole mount *in situ* RNA hybridization according to the protocol of Thisse *et al.* (1993). A probe for *tyrosinase related protein 2/dct* (Kelsh *et al.*, 2000) was generated from a linearized plasmid template transcribed with T7 RNA polymerase (Stratagene, La Jolla, CA). To label dying cells, embryos were incubated in 5 μg/ml AO (Sigma, St Louis, MO) diluted in fish water for 30 minutes, then washed three times

for 10 minutes each on a rotating platform, and examined with fluorescent microscopy.

Drugs

zVAD-fmk (Enzyme Systems Product; Livermore, CA) or the negative control compound zFA-fmk was applied at 200 μM in fish water (Westerfield, 1993). A saturated solution of PTU (Sigma) (Milos and Dingle, 1978) was diluted 100-fold in fish water before being applied to embryos at 24 hpf. Camptothecin (Sigma) was diluted to 1 μM from a stock made in DMSO.

Transmission electron microscopy

At 48 hpf *trpm7* mutant and 5 dpf *kit* mutant animals were fixed overnight in 1.5% glutaraldehyde and 1.6% paraformaldehyde (Electron Microscopy Sciences; Hatfield, PA) in 100 mM sodium cacodylate buffer. Embryos were postfixed with 1% osmium tetroxide and 1.5% potassium ferrocyanide in 100 mM sodium cacodylate buffer, then *en bloc* stained with 2.5% uranyl acetate and dehydrated in a graded ethanol series. Samples were transitioned into propylene oxide (EM Science; Cheery Hill, NJ) to preserve melanosome integrity and embedded in Epon 812 resin (Ted Pella; Redding, CA). Polymerized blocks were sectioned at 1 μm intervals using a diamond histology knife (Diatome; Biel, Switzerland) and collected serially upon precleaned glass slides (Surgipathy; Richmond, IL). Using a Leica DMRA2 microscope (Leica Microsystems, Germany), individual sections were selected for the presence of one or more melanophores and subsequently re-embedded in Epon 812 resin. Sections (1 μm) were cut for transmission electron microscopy and collected on formvar-coated grids. Sections were post-section stained with 2.5% uranyl acetate and Reynold's lead citrate, and then examined using a Jeol JEM-1230 electron microscope (Reynolds, 1963). After image capture, visible dirt was erased from extracellular spaces using tools in Adobe Photoshop Elements 4.0 (Adobe, San Jose, CA).

Microscopy

Bright field and epifluorescence micrographs were captured on a Leica DMRA2 compound microscope or a Leica MZ FLIII stereo microscope (Leica Microsystems), with a Retiga 1300 digital camera (Q-Imaging, Burnaby, BC, Canada) and Openlab software (Improvision, Lexington, MA). Contrast and sharpness were manipulated in Adobe Photoshop. In quantitative analyses of melanophores, they were counted on the dorsum, between the most caudal part of the eye and the point where the hindbrain constricts to become the spinal cord. To calculate percentage rescue, we first subtracted the number of melanophores in untreated mutants from the number in treated mutants, then divided by the number in wild-type animals, and multiplied by 100.

Tissue culture

The isolation and culture of normal melanocytes (FM13), keratinocytes (FK10), and dermal fibroblasts (DF1) was performed as described previously (Hsu and Herlyn, 1996; Hsu *et al.*, 1998). Melanoma cell lines, including primary (WM983C) and metastatic (WM1205Lu), were maintained as described (Hsu *et al.*, 1999). The metastatic melanoma cell line, A375P, and its aggressive/invasive variants, A375M, A375P-5, and A375P-10 were derived and maintained as described (Seftor *et al.*, 1990). Total messenger RNA was prepared using RNAqueous®-4PCR (Ambion, Austin, TX) according to the manufacturer's protocol.

Quantitative RT-PCR

RNA concentrations were determined using a SmartSpec Plus spectrophotometer (Bio-Rad Laboratories, Hercules, CA) and diluted to maximum concentrations of 1 mg/ml. For complementary DNA (cDNA) reactions, 200 ng of total RNA was added to 0.5 μg random hexamers DNA primers plus 2.5 μl of 10 mM dNTPs (Invitrogen; Carlsbad, CA), and brought to 30 μl with nuclease-free water. Reactions were heated to 65°C for 5 minutes, and cooled to 4.0°C for 5 minutes in a PTC-200 Peltier Thermo Cycler (MJ Research; Ramsey, MN). We then added 15 μl of a master mix containing 10 μl of 5 × First-Strand buffer (Invitrogen), 5 μl of 0.1 M dithiothreitol, 20 units of RNasin (Promega, Madison, WI), and nuclease-free water to a volume of 15 μl. Reactions were incubated at 25°C for 10 minutes, followed by 37°C for 2 minutes. Then 5 μl of a mix composed of 4 μl master mix and either 1 μl Moloney-murine leukemia virus Reverse Transcriptase (New England Biolabs, Ipswich, MA) or 1 μl nuclease-free water was added to each reaction. Total reactions were incubated at 37°C for 50 minutes followed by 70°C for 15 minutes. PCR reactions (25 μl) were prepared with approximately 10 ng of cDNA using the SYBR Green kit (Applied Biosystems, Foster City, CA) following the manufacturer's instructions. The following primers were at a final concentration of 200 nM in separate PCR reactions: human *TRPM7* (forward: GCC ACT TGG AAA CTG GAA CC; reverse: CGGTAGATGG CCTTCTACTG), human *TRPM1* (forward: CACCCAGAGCTACC CAACAGA; reverse: CGGATATACATGGCTTTATTGGAA) or human 18S ribosomal cDNA (forward: GATGGGCGGCGGAAAATAG; reverse: GCGTGGATTCTGCATAATGGT). Quantitative real-time PCR in 96-well plates (Applied Biosystems) was conducted, using an Applied Biosystems Model 7000 thermal cycler and following the default protocol and using SDS software version 1.2.3 and the standard curve method described in the user manual to calculate relative messenger RNA expression levels (also see Bookout and Mangelsdorf, 2003). Additional reactions included a non-template control using solutions from cDNA reactions run without reverse transcriptase, and a dissociation curve at the end of the program. We generated standard curves for *TRPM7*, *TRPM1*, and their *18S* normalizing controls from 10-fold dilutions of DF1 fibroblast cDNA (*TRPM7* reactions and *18S* control; slopes: −3.47 and −3.43, respectively) or WM983C melanoma cDNA (*TRPM1* reactions and *18S* control; slopes: −3.715 and −3.124, respectively). Standard curves and experimental reactions were run in duplicate and triplicate, respectively. *TRPM7* message levels were measured twice with similar results.

CONFLICT OF INTEREST

The authors state no conflict of interest.

ACKNOWLEDGMENTS

We are grateful to Thomas Look for plasmids, members of Frederick Domann's laboratory for help with quantitative PCR. We are grateful to Paul Henion, David Parichy, and Michael Elizondo for productive discussions, and to Brigitte Arduini and Michael Elizondo for repeating calcium-mediated rescue of melanophores in *trpm7* mutants in their respective laboratories. We acknowledge early efforts on this project from Jaime Sabel. This work was supported by a seed grant to RAC from the American Cancer Society,

administered by the Holden Comprehensive Cancer Care Center, and NIH GM067841 to RAC.

REFERENCES

Aarts MM, Tymianski M (2005) TRPMs and neuronal cell death. *Pflugers Arch* 451:243–9

Anderson DM, Lyman SD, Baird A, Wignall JM, Eisenman J, Rauch C *et al.* (1990) Molecular cloning of mast cell growth factor, a hematopoietin that is active in both membrane bound and soluble forms. *Cell* 63:235–43

Arduini BL, Henion PD (2004) Melanophore sublineage-specific requirement for zebrafish touchtone during neural crest development. *Mech Dev* 121:1353–64

Assuncao Guimaraes C, Linden R (2004) Programmed cell deaths. Apoptosis and alternative deathstyles. *Eur J Biochem* 271:1638–50

Baxter LL, Hou L, Loftus SK, Pavan WJ (2004) Spotlight on spotted mice: a review of white spotting mouse mutants and associated human pigmentation disorders. *Pigment Cell Res* 17:215–24

Boissy RE, Manga P (2004) On the etiology of contact/occupational vitiligo. *Pigment Cell Res* 17:208–14

Bookout AL, Mangelsdorf DJ (2003) Quantitative real-time PCR protocol for analysis of nuclear receptor signaling pathways. *Nucl Recept Signal* 1:e012

Busam KJ, Wolchok J, Jungbluth AA, Chapman P (2004) Diffuse melanosis after chemotherapy-induced tumor lysis syndrome in a patient with metastatic melanoma. *J Cutan Pathol* 31:274–80

Chen KG, Valencia JC, Lai B, Zhang G, Paterson JK, Rouzaud F *et al.* (2006) Melanosomal sequestration of cytotoxic drugs contributes to the intractability of malignant melanomas. *Proc Natl Acad Sci USA* 103:9903–7

Clark K, Langeslag M, van Leeuwen B, Ran L, Ryazanov AG, Figdor CG *et al.* (2006) TRPM7, a novel regulator of actomyosin contractility and cell adhesion. *EMBO J* 25:290–301

Cole LK, Ross LS (2001) Apoptosis in the developing zebrafish embryo. *Dev Biol* 240:123–42

Cools AR (1972) Asymmetrical spotting and direction of circling in the varitint-waddler mouse. *J Hered* 63:167–71

Cornell RA, Yemm E, Bonde G, Li W, d'Alencon C, Wegman L *et al.* (2004) Touchtone promotes survival of embryonic melanophores in zebrafish. *Mech Dev* 121:1365–76

Di Palma F, Belyantseva IA, Kim HJ, Vogt TF, Kachar B, Noben-Trauth K (2002) Mutations in Mcoln3 associated with deafness and pigmentation defects in varitint-waddler (Va) mice. *Proc Natl Acad Sci USA* 99:14994–9

Duncan LM, Deeds J, Hunter J, Shao J, Holmgren LM, Woolf EA *et al.* (1998) Down-regulation of the novel gene melastatin correlates with potential for melanoma metastasis. *Cancer Res* 58:1515–20

Dutton KA, Pauliny A, Lopes SS, Elworthy S, Carney TJ, Rauch J *et al.* (2001) Zebrafish colourless encodes sox10 and specifies non-ectomesenchymal neural crest fates. *Development* 128:4113–25

Elizondo MR, Arduini BL, Paulsen J, MacDonald EL, Sabel JL, Henion PD *et al.* (2005) Defective skeletogenesis with kidney stone formation in dwarf zebrafish mutant for trpm7. *Curr Biol* 15:667–71

Giraldez AJ, Cinalli RM, Glasner ME, Enright AJ, Thomson JM, Baskerville S *et al.* (2005) MicroRNAs regulate brain morphogenesis in zebrafish. *Science* 308:833–8

Gritsman K, Zhang J, Cheng S, Heckscher E, Talbot WS, Schier AF (1999) The EGF-CFC protein one-eyed pinhead is essential for nodal signaling. *Cell* 97:121–32

Hanano T, Hara Y, Shi J, Morita H, Umebayashi C, Mori E *et al.* (2004) Involvement of TRPM7 in cell growth as a spontaneously activated Ca2+ entry pathway in human retinoblastoma cells. *J Pharmacol Sci* 95:403–19

Harteneck C (2005) Function and pharmacology of TRPM cation channels. *Naunyn Schmiedebergs Arch Pharmacol* 371:307–14

He Y, Yao G, Savoia C, Touyz RM (2005) Transient receptor potential melastatin 7 ion channels regulate magnesium homeostasis in vascular smooth muscle cells: role of angiotensin II. *Circ Res* 96:207–15

Hemesath TJ, Price ER, Takemoto C, Badalian T, Fisher DE (1998) MAP kinase links the transcription factor microphthalmia to c-Kit signalling in melanocytes. *Nature* 391:298–301

Hermosura MC, Nayakanti H, Dorovkov MV, Calderon FR, Ryazanov AG, Haymer DS *et al.* (2005) A TRPM7 variant shows altered sensitivity to magnesium that may contribute to the pathogenesis of two Guamanian neurodegenerative disorders. *Proc Natl Acad Sci USA* 102: 11510–5

Hochstein P, Cohen G (1963) The cytotoxicity of melanin precursors. *Ann NY Acad Sci* 100:876–86

Hsu M-Y, Herlyn M (1996) Cultivation of normal human epidermal melanocytes. In: *Human Cell Culture Protocols.* (Jones General, ed), Totowa, NJ: Humana Press, pp 9–20

Hsu MY, Shih DT, Meier FE, Van Belle P, Hsu JY, Elder DE *et al.* (1998) Adenoviral gene transfer of beta3 integrin subunit induces conversion from radial to vertical growth phase in primary human melanoma. *Am J Pathol* 153:1435–42

Huang CL, Nordlund JJ, Boissy R (2002) Vitiligo: a manifestation of apoptosis? *Am J Clin Dermatol* 3:301–8

Johnson R, Jackson IJ (1992) Light is a dominant mouse mutation resulting in premature cell death. *Nat Genet* 1:226–9

Kane DA, McFarland KN, Warga RM (2005) Mutations in half baked/E-cadherin block cell behaviors that are necessary for teleost epiboly. *Development* 132:1105–16

Kelsh RN, Brand M, Jiang YJ, Heisenberg CP, Lin S, Haffter P *et al.* (1996) Zebrafish pigmentation mutations and the processes of neural crest development. *Development* 123:369–89

Kelsh RN, Schmid B, Eisen JS (2000) Genetic analysis of melanophore development in zebrafish embryos. *Dev Biol* 225:277–93

Kerr JF, Wyllie AH, Currie AR (1972) Apoptosis: a basic biological phenomenon with wide-ranging implications in tissue kinetics. *Br J Cancer* 26:239–57

Kimmel CB, Ballard WW, Kimmel SR, Ullmann B, Schilling TF (1995) Stages of embryonic development of the zebrafish. *Dev Dyn* 203:253–310

Krapivinsky G, Mochida S, Krapivinsky L, Cibulsky SM, Clapham DE (2006) The TRPM7 ion channel functions in cholinergic synaptic vesicles and affects transmitter release. *Neuron* 52:485–96

Kunert-Keil C, Bisping F, Kruger J, Brinkmeier H (2006) Tissue-specific expression of TRP channel genes in the mouse and its variation in three different mouse strains. *BMC Genomics* 7:159

Lamason RL, Mohideen MA, Mest JR, Wong AC, Norton HL, Aros MC *et al.* (2005) SLC24A5, a putative cation exchanger, affects pigmentation in zebrafish and humans. *Science* 310:1782–6

Langheinrich U, Hennen E, Stott G, Vacun G (2002) Zebrafish as a model organism for the identification and characterization of drugs and genes affecting p53 signaling. *Curr Biol* 12:2023–8

Lister JA, Robertson CP, Lepage T, Johnson SL, Raible DW (1999) nacre encodes a zebrafish microphthalmia-related protein that regulates neural-crest-derived pigment cell fate. *Development* 126:3757–67

Liu TX, Howlett NG, Deng M, Langenau DM, Hsu K, Rhodes J *et al.* (2003) Knockdown of zebrafish Fancd2 causes developmental abnormalities via p53-dependent apoptosis. *Dev Cell* 5:903–14

Lynn Lamoreux M, Kelsh RN, Wakamatsu Y, Ozato K (2005) Pigment pattern formation in the medaka embryo. *Pigment Cell Res* 18:64–73

Mastore M, Kohler L, Nappi AJ (2005) Production and utilization of hydrogen peroxide associated with melanogenesis and tyrosinase-mediated oxidations of DOPA and dopamine. *FEBS J* 272:2407–15

McGill GG, Horstmann M, Widlund HR, Du J, Motyckova G, Nishimura EK *et al.* (2002) Bcl2 regulation by the melanocyte master regulator Mitf modulates lineage survival and melanoma cell viability. *Cell* 109: 707–18

McNulty S, Fonfria E (2005) The role of TRPM channels in cell death. *Pflugers Arch* 451:235–42

Miller AJ, Du J, Rowan S, Hershey CL, Widlund HR, Fisher DE (2004) Transcriptional regulation of the melanoma prognostic marker melastatin (TRPM1) by MITF in melanocytes and melanoma. *Cancer Res* 64: 509–16

Miller BA (2006) The role of TRP channels in oxidative stress-induced cell death. *J Membr Biol* 209:31–41

Milos N, Dingle AD (1978) Dynamics of pigment pattern formation in the zebrafish brachydanio rerio. I. Establishment and regulation of the lateral line melanophore stripe during the first eight days of development. *J Exp Zool* 205:205–16

Moridani MY, Cheon SS, Khan S, O'Brien PJ (2002) Metabolic activation of 4-hydroxyanisole by isolated rat hepatocytes. *Drug Metab Dispos* 30:1063–9

Monteilh-Zoller MK, Hermosura MC, Nadler MJ, Scharenberg AM, Penner R, Fleig, A (2003) TRPM7 provides as ion channel mechanism for cellular entry of trace metal ions. *J Gen Physiol* 121:49–60

Nadler MJ, Hermosura MC, Inabe K, Perraud AL, Zhu Q, Stokes AJ *et al.* (2001) LTRPC7 is a Mg. ATP-regulated divalent cation channel required for cell viability. *Nature* 411:590–5

Nicotera P, Melino G (2004) Regulation of the apoptosis-necrosis switch. *Oncogene* 23:2757–65

Page-McCaw PS, Chung SC, Muto A, Roeser T, Staub W, Finger-Baier KC *et al.* (2004) Retinal network adaptation to bright light requires tyrosinase. *Nat Neurosci* 7:1329–36

Parichy DM, Rawls JF, Pratt SJ, Whitfield TT, Johnson SL (1999) Zebrafish sparse corresponds to an orthologue of c-kit and is required for the morphogenesis of a subpopulation of melanocytes, but is not essential for hematopoiesis or primordial germ cell development. *Development* 126:3425–36

Pawelek JM, Lerner AB (1978) 5,6-Dihydroxyindole is a melanin precursor showing potent cytotoxicity. *Nature* 276:626–8

Postlethwait JH, Johnson SL, Midson CN, Talbot WS, Gates M, Ballinger EW *et al.* (1994) A genetic linkage map for the zebrafish. *Science* 264: 699–703

Ramsey IS, Delling M, Clapham DE (2006) An introduction to TRP channels. *Annu Rev Physiol* 68:619–47

Reynolds ES (1963) The use of lead citrate at high pH as an electron-opaque stain in electron microscopy. *J Cell Biol* 17:208–12

Riley PA (1998) Mechanisms of inhibition of melanin pigmentation. In: *The Pigmentary System: Physiology and Pathophysiology*. (Nordlund JJ, Boissy RE, Hearing VJ, King RA and Ortonne J-P, eds), New York: Oxford University Press

Riley PA (2003) Melanogenesis and melanoma. *Pigment Cell Res* 16:548–52

Rizzuto R, Pinton P, Ferrari D, Chami M, Szabadkai G, Magalhaes PJ *et al.* (2003) Calcium and apoptosis: facts and hypotheses. *Oncogene* 22:8619–27

Sanders LH, Whitlock KE (2003) Phenotype of the zebrafish masterblind (mbl) mutant is dependent on genetic background. *Dev Dyn* 227:291–300

Scharenberg AM (2005) TRPM2 and TRPM7: channel/enzyme fusions to generate novel intracellular sensors. *Pflugers Arch* 451:220–7

Schmitz C, Perraud AL, Johnson CO, Inabe K, Smith MK, Penner R *et al.* (2003) Regulation of vertebrate cellular Mg2+ homeostasis by TRPM7. *Cell* 114:191–200

Seftor EA, Seftor RE, Hendrix MJ (1990) Selection of invasive and metastatic subpopulations from a heterogeneous human melanoma cell line. *Biotechniques* 9:324–31

Smit N, Tilgmann C, Karhunen T, Slingerland R, Ulmanen I, Westerhof W *et al.* (1994) O-methylation of L-dopa in melanin metabolism and the presence of catechol-O-methyltransferase in melanocytes. *Pigment Cell Res* 7:403–8

Spritz RA (2006) The genetics of generalized vitiligo and associated autoimmune diseases. *J Dermatol Sci* 41:3–10

Streisinger G, Walker C, Dower N, Knauber D, Singer F (1981) Production of clones of homozygous diploid zebra fish (Brachydanio rerio). *Nature* 291:293–6

Su LT, Agapito MA, Li M, Simonson WT, Huttenlocher A, Habas R *et al.* (2006) TRPM7 regulates cell adhesion by controlling the calcium-dependent protease calpain. *J Biol Chem* 281:11260–70

Thisse B, Pflumio S, Furthauer M, Loppin B, Heyer V, Degrave A *et al.* (2001) Expression of the zebrafish genome during embryogenesis. *ZFIN Direct Data Submission ZFINID:ZDB-PUB-010810-1*

Thisse C, Thisse B, Schilling TF, Postlethwait JH (1993) Structure of the zebrafish snail1 gene and its expression in wild-type, spadetail and no tail mutant embryos. *Development* 119:1203–15

Westerfield M (1993) *The zebrafish book*. Eugene, OR: University of Oregon Press

Williams JA, Barrios A, Gatchalian C, Rubin L, Wilson SW, Holder N (2000) Programmed cell death in zebrafish rohon beard neurons is influenced by TrkC1/NT-3 signaling. *Dev Biol* 226:220–30

Williams JA, Holder N (2000) Cell turnover in neuromasts of zebrafish larvae. *Hear Res* 143:171–81

Wolf FI (2004) TRPM7: channeling the future of cellular magnesium homeostasis? *Sci STKE* 2004:pe23

Yang CT, Johnson SL (2006) Small molecule-induced ablation and subsequent regeneration of larval zebrafish melanocytes. *Development* 133:3563–73

Yang F, Sarangarajan R, Le Poole IC, Medrano EE, Boissy RE (2000) The cytotoxicity and apoptosis induced by 4-tertiary butylphenol in human melanocytes are independent of tyrosinase activity. *J Invest Dermatol* 114:157–64

Zhiqi S, Soltani MH, Bhat KM, Sangha N, Fang D, Hunter JJ *et al.* (2004) Human melastatin 1 (TRPM1) is regulated by MITF and produces multiple polypeptide isoforms in melanocytes and melanoma. *Melanoma Res* 14:509–16